

# Electrically pumped continuous-wave 1.3 $\mu\text{m}$ InAs/GaAs quantum dot lasers monolithically grown on on-axis Si (001) substrates

SIMING CHEN,<sup>1,\*</sup> MENGYA LIAO,<sup>1</sup> MINGCHU TANG,<sup>1</sup> JIANG WU,<sup>1</sup> MICKAEL MARTIN,<sup>2</sup> THIERRY BARON,<sup>2</sup> ALWYN SEEDS,<sup>1</sup> AND HUIYUN LIU<sup>1</sup>

<sup>1</sup>Department of Electronic and Electrical Engineering, University College London, London, WC1E 7JE, UK

<sup>2</sup>Univ. Grenoble Alpes, CNRS, CEA-LETI, MINATEC, LTM, F-38054 Grenoble, France

\*[siming.chen@ucl.ac.uk](mailto:siming.chen@ucl.ac.uk)

**Abstract:** We report on the first electrically pumped continuous-wave (cw) InAs/GaAs quantum dot (QD) lasers monolithically grown on on-axis Si (001) substrates without any intermediate buffer layers. A 400 nm antiphase boundary (APB) free epitaxial GaAs film with a small root-mean-square (RMS) surface roughness of 0.86 nm was first deposited on a 300 mm standard industry-compatible on-axis Si (001) substrate by metal-organic chemical vapor deposition (MOCVD). The QD laser structure was then grown on this APB-free GaAs/Si (001) virtual substrate by molecular beam epitaxy (MBE). Room-temperature cw lasing at  $\sim 1.3 \mu\text{m}$  has been achieved with a threshold current density of  $425 \text{ A/cm}^2$  and single facet output power of 43 mW. Under pulsed operation, lasing operation up to  $102 \text{ }^\circ\text{C}$  has been realized, with a threshold current density of  $250 \text{ A/cm}^2$  and single facet output power exceeding 130 mW at room temperature.

Published by The Optical Society under the terms of the [Creative Commons Attribution 4.0 License](https://creativecommons.org/licenses/by/4.0/). Further distribution of this work must maintain attribution to the author(s) and the published article's title, journal citation, and DOI.

**OCIS codes:** (230.5590) Quantum-well, -wire and -dot devices; (250.5960) Semiconductor lasers; (250.5300) Photonic integrated circuits.

## References and links

1. M. Asghari and A. V. Krishnamoorthy, "Silicon photonics: Energy-efficient communication," *Nat. Photonics* **5**(5), 268–270 (2011).
2. A. Rickman, "The commercialization of silicon photonics," *Nat. Photonics* **8**(8), 579–582 (2014).
3. D. Liang and J. E. Bowers, "Recent progress in lasers on silicon," *Nat. Photonics* **4**(8), 511–517 (2010).
4. S. Tanaka, S. H. Jeong, S. Sekiguchi, T. Kurahashi, Y. Tanaka, and K. Morito, "High-output-power, single-wavelength silicon hybrid laser using precise flip-chip bonding technology," *Opt. Express* **20**(27), 28057–28069 (2012).
5. H. H. Chang, A. W. Fang, M. N. Sysak, H. Park, R. Jones, O. Cohen, O. Raday, M. J. Paniccia, and J. E. Bowers, "1310nm silicon evanescent laser," *Opt. Express* **15**(18), 11466–11471 (2007).
6. Y.-H. Jhang, R. Mochida, K. Tanabe, K. Takemasa, M. Sugawara, S. Iwamoto, and Y. Arakawa, "Direct modulation of 1.3  $\mu\text{m}$  quantum dot lasers on silicon at  $60 \text{ }^\circ\text{C}$ ," *Opt. Express* **24**(16), 18428–18435 (2016).
7. Z. Zhou, B. Yin, and J. Michel, "On-chip light sources for silicon photonics," *Light Sci. Appl.* **4**(11), e358 (2015).
8. E. Tourmié, L. Cerutti, J. B. Rodriguez, H. Liu, J. Wu, and S. Chen, "Metamorphic III–V semiconductor lasers grown on silicon," *MRS Bull.* **41**(3), 223–233 (2016).
9. J. Wu, S. Chen, A. Seeds, and H. Liu, "Quantum dot optoelectronic devices: lasers, photodetectors and solar cells," *J. Phys. D Appl. Phys.* **48**(36), 363001 (2015).
10. D. G. Deppe, K. Shavritranuruk, G. Ozgur, H. Chen, and S. Freisem, "Quantum dot laser diode with low threshold and low internal loss," *Electron. Lett.* **45**(1), 54–56 (2009).
11. Y. Arakawa and H. Sakaki, "Multidimensional quantum well laser and temperature dependence of its threshold current," *Appl. Phys. Lett.* **40**(11), 939–941 (1982).
12. M. Sugawara and M. Usami, "Quantum dot devices: handing the heat," *Nat. Photonics* **3**(1), 30–31 (2009).
13. T. Wang, H. Liu, A. Lee, F. Pozzi, and A. Seeds, "1.3- $\mu\text{m}$  InAs/GaAs quantum-dot lasers monolithically grown on Si substrates," *Opt. Express* **19**(12), 11381–11386 (2011).

14. M. Tang, S. Chen, J. Wu, Q. Jiang, V. G. Dorogan, M. Benamara, Y. I. Mazur, G. J. Salamo, A. Seeds, and H. Liu, "1.3- $\mu\text{m}$  InAs/GaAs quantum-dot lasers monolithically grown on Si substrates using InAlAs/GaAs dislocation filter layers," *Opt. Express* **22**(10), 11528–11535 (2014).
15. A. Y. Liu, C. Zhang, J. Norman, A. Snyder, D. Lubyshev, J. M. Fastenau, A. W. Liu, A. C. Gossard, and J. E. Bowers, "High performance continuous wave 1.3  $\mu\text{m}$  quantum dot lasers on silicon," *Appl. Phys. Lett.* **104**(4), 041104 (2014).
16. S. Chen, M. Tang, Q. Jiang, J. Wu, V. G. Dorogan, M. Benamara, Y. I. Mazur, G. J. Salamo, P. Smowton, A. Seeds, and H. Liu, "InAs/GaAs quantum-dot superluminescent light-emitting diode monolithically grown on a Si Substrate," *ACS Photonics* **1**(7), 638–642 (2014).
17. M. Tang, S. Chen, J. Wu, Q. Jiang, K. Kennedy, P. Jurczak, M. Liao, R. Beanland, A. Seeds, and H. Liu, "Optimizations of Defect Filter Layers for 1.3- $\mu\text{m}$  InAs/GaAs Quantum-Dot Lasers Monolithically Grown on Si Substrates," *IEEE J. Sel. Top. Quantum Electron.* **22**(6), 1900207 (2016).
18. Q. Jiang, M. Tang, S. Chen, J. Wu, A. Seeds, and H. Liu, "InAs/GaAs quantum-dot superluminescent diodes monolithically grown on a Ge substrate," *Opt. Express* **22**(19), 23242–23248 (2014).
19. H. Liu, T. Wang, Q. Jiang, R. Hogg, F. Tutu, F. Pozzi, and A. Seeds, "Long-wavelength InAs/GaAs quantum dot laser diode monolithically grown on Ge substrate," *Nat. Photonics* **5**(7), 416–419 (2011).
20. A. Y. Liu, R. W. Herrick, O. Ueda, P. M. Petroff, A. C. Gossard, and J. E. Bowers, "Bowers, "Reliability of InAs/GaAs Quantum Dot Lasers Epitaxially Grown on Silicon," *IEEE J. Sel. Top. Quantum Electron.* **21**(6), 1900708 (2015).
21. A. Y. Liu, S. Srinivasan, J. Norman, A. C. Gossard, and E. J. Bowers, "Quantum dot lasers for silicon photonics [Invited]," *Photonics Res.* **3**(5), B1–B9 (2015).
22. Z. Mi, J. Yang, P. Bhattacharya, G. Qin, and Z. Ma, "High-performance quantum dot lasers and integrated optoelectronics on Si," *Proc. IEEE* **97**(7), 1239–1249 (2009).
23. S. Chen, M. Tang, J. Wu, Q. Jiang, V. G. Dorogan, M. Benamara, Y. I. Mazur, G. J. Salamo, A. Seeds, and H. Liu, "1.3  $\mu\text{m}$  InAs/GaAs quantum-dot laser monolithically grown on Si substrates operating over 100  $^{\circ}\text{C}$ ," *Electron. Lett.* **50**(20), 1467–1468 (2014).
24. S. Chen, W. Li, J. Wu, Q. Jiang, M. Tang, S. Shutts, S. Elliott, A. Sobiesierski, A. Seeds, I. Ross, P. Smowton, and H. Liu, "Electrically pumped continuous-wave III–V quantum dot lasers on silicon," *Nat. Photonics* **10**(5), 307–311 (2016).
25. R. Fischer, W. T. Masselink, J. Klem, T. Henderson, T. C. McGlenn, M. V. Klein, H. Morkoç, J. H. Mazur, and J. Washburn, "Growth and properties of GaAs/AlGaAs on nonpolar substrates using molecular beam epitaxy," *J. Appl. Phys.* **58**(1), 374–381 (1985).
26. M. Akiyama, Y. Kawarada, T. Ueda, S. Nishi, and K. Kaminishi, "Growth of high quality GaAs layers on Si substrates by MOCVD," *J. Cryst. Growth* **77**(1–3), 490–497 (1986).
27. K. Volz, A. Beyer, W. Witte, J. Ohlmann, I. Nemeth, B. Kunert, and W. Stolz, "GaP-nucleation on exact Si (0 0 1) substrates for III/V device integration," *J. Cryst. Growth* **315**(1), 37–47 (2011).
28. D. Jung, Y. Song, M. Lee, T. Masuda, and X. Huang, "InGaAs/GaAs quantum well lasers grown on exact gap/Si (001)," *Electron. Lett.* **50**(17), 1226–1227 (2014).
29. Y. Wan, Q. Li, A. Y. Liu, A. C. Gossard, J. E. Bowers, E. L. Hu, and K. M. Lau, "Optically pumped 1.3  $\mu\text{m}$  room-temperature InAs quantum-dot micro-disk lasers directly grown on (001) silicon," *Opt. Lett.* **41**(7), 1664–1667 (2016).
30. A. Y. Liu, J. Peters, X. Huang, D. Jung, J. Norman, M. L. Lee, A. C. Gossard, and J. E. Bowers, "Electrically pumped continuous-wave 1.3  $\mu\text{m}$  quantum-dot lasers epitaxially grown on on-axis (001) GaP/Si," *Opt. Lett.* **42**(2), 338–341 (2017).
31. R. Alcotte, M. Martin, J. Moeyaert, R. Cipro, S. David, F. Bassani, F. Ducroquet, Y. Bogumilowicz, E. Sanchez, Z. Ye, X. Bao, J. Pin, and T. Baron, "Epitaxial growth of antiphase boundary free GaAs layer on 300 mm Si (001) substrate by metalorganic chemical vapour deposition with high mobility," *APL Mater.* **4**(4), 046101 (2016).
32. J. R. Orchard, S. Shutts, A. Sobiesierski, J. Wu, M. Tang, S. Chen, Q. Jiang, S. Elliott, R. Beanland, H. Liu, P. M. Smowton, and D. J. Mowbray, "In situ annealing enhancement of the optical properties and laser device performance of InAs quantum dots grown on Si substrates," *Opt. Express* **24**(6), 6196–6202 (2016).
33. H. W. Yu, E. Y. Chang, Y. Yamamoto, B. Tillack, W. C. Wang, C. I. Kuo, Y. Y. Wong, and H. Q. Nguyen, "Effect of graded-temperature arsenic prelayer on quality of GaAs on Ge/Si substrates by metalorganic vapor phase epitaxy," *Appl. Phys. Lett.* **99**(17), 171908 (2011).
34. X. Zhou, J. Pan, R. Liang, J. Wang, and W. Wang, "Epitaxy of GaAs thin film with low defect density and smooth surface on Si substrate," *J. Semicond.* **35**(7), 073002 (2014).
35. A. Beyer, I. Németh, S. Liebich, J. Ohlmann, W. Stolz, and K. Volz, "Influence of crystal polarity on crystal defects in GaP grown on exact Si (001)," *J. Appl. Phys.* **109**(8), 083529 (2011).
36. O. Shechekin and D. Deppe, "1.3  $\mu\text{m}$  InAs quantum dot laser with  $T_0 = 161$  K from 0 to 80  $^{\circ}\text{C}$ ," *Appl. Phys. Lett.* **80**(18), 3277–3279 (2002).

## 1. Introduction

Driven by cloud-based applications, 'big-data' services and enterprise data centers, silicon photonics has become of increased interest due to its potential prospects for integration of

optical data transfer with data processing electronics on a single silicon die utilizing CMOS-compatible IC technology [1, 2]. However, such integration is currently incomplete due to the lack of a reliable, directly integrable Si-based laser optical source [3]. Although wafer-bonding and flip-chip-bonding have been extensively investigated for integrating III-V lasers into silicon photonics platforms, and impressive results have been achieved [4–6]; In the longer term, monolithic growth of III-V lasers on Si substrates remains the ‘holy grail’ for low-cost, high yield, and large-scale integration of complex optoelectronic circuits [7, 8]. However, direct epitaxial growth of III-V materials on Si substrates faces several significant challenges including large lattice mismatch, different thermal expansion coefficients and polar III-V versus non-polar Si surfaces, which induce the formation of different types of defects, such as threading dislocations (TDs), micro thermal cracks and antiphase boundaries (APBs), respectively. These defects all generate non-radiative recombination centers, which will dramatically reduce the quality of III-V materials as well as the operating performance and lifetime of devices fabricated from them [3, 9]. Quantum dots (QDs) have been becoming the main technology as active layers in semiconductor lasers due to their low threshold current density and temperature insensitive operation [10–12]. In addition, QD structures have attracted increasing attention for the active element of III-V light emitting sources on silicon substrates [13–18], due to their enhanced tolerance to defects [19–22].

Pioneering work on 1.3  $\mu\text{m}$  InAs/GaAs QD lasers monolithically grown on Si substrates has demonstrated impressive results [15, 23, 24]. In order to prevent the emergence of the APBs while growing polar III-V materials on non-polar silicon substrates, silicon (001) or equivalent orientation substrates with an offcut of 4–6° [25, 26] to the [110] plane have been used to form a perfect double silicon atom step. Although this approach is successful in overcoming the APB problem, it has the disadvantage of not being readily compatible with standard microelectronics fabrication, where wafers with nominally (001) silicon substrates are used. In general, the nominal silicon substrates, i.e., the so-called “exact” (001) silicon substrates with a miscut angle less than 0.5° [8, 27], have been used in standard microelectronics fabrication. To this end, there has been notable progress made to achieve lasing operation from on-axis Si (001) substrates, including the demonstrations of electrically pumped 1  $\mu\text{m}$  InGaAs/GaAs quantum well lasers grown on GaP/Si (001) substrates under pulsed operation [28], optically pumped cw 1.3  $\mu\text{m}$  InAs QD microdisk lasers grown on patterned (001) silicon substrates [29] and electrically pumped cw 1.3  $\mu\text{m}$  InAs QD edge-emitting lasers epitaxially grown on GaP/Si (001) substrates [30]. However, for these techniques, either patterned Si substrates or an intermediate GaP buffer has to be used. Furthermore, QD lasers directly grown on GaAs/Si (001) substrates have not yet been reported. In this paper, we report on, to the best of our knowledge, the first electrically pumped cw 1.3  $\mu\text{m}$  InAs/GaAs QD lasers directly grown on microelectronics standard nominal (001) Si substrates without any intermediate buffers.

## 2. Experimental procedure

### 2.1 Crystal growth

In this work, microelectronics standard on-axis Si (001) 300 mm diameter wafers were deoxidized by the SiConi process using a  $\text{NF}_3/\text{NH}_3$  remote plasma. The wafers were then transferred into a 300 mm Applied Materials metalorganic chemical vapour deposition (MOCVD) reactor, where  $\text{H}_2$  annealing was performed at 900 °C to promote structuring of the  $2 \times 1$  surface using purified  $\text{H}_2$  as the carrier gas. After the annealing process, the chamber was quickly quenched below 700 °C within 30 s to freeze the silicon surface structure. GaAs layers were then grown sequentially, with a standard two-step process [31]: a 40 nm GaAs nucleation layer was deposited at low temperature (400–500 °C); a 360 nm GaAs layer was then deposited at a higher temperature (600–700 °C). The typical V/III ratio was in the range of 5–30. The temperatures were monitored by an optical pyrometer. After completion of the epitaxial growth of 400 nm APB-free GaAs films on the 300 mm silicon (001) wafer, it was



### 2.3 Measurements

The surface morphology was characterized by a Nanoscope Dimension 3100 SPM atomic force microscopy (AFM) system using a standard tapping mode. Optical properties were measured by photoluminescence (PL) measurements excited from a 635 nm diode-pumped solid-state laser. Laser device characteristics were measured under both cw and pulsed conditions of 1  $\mu$ s pulse-width and 1% duty-cycle.

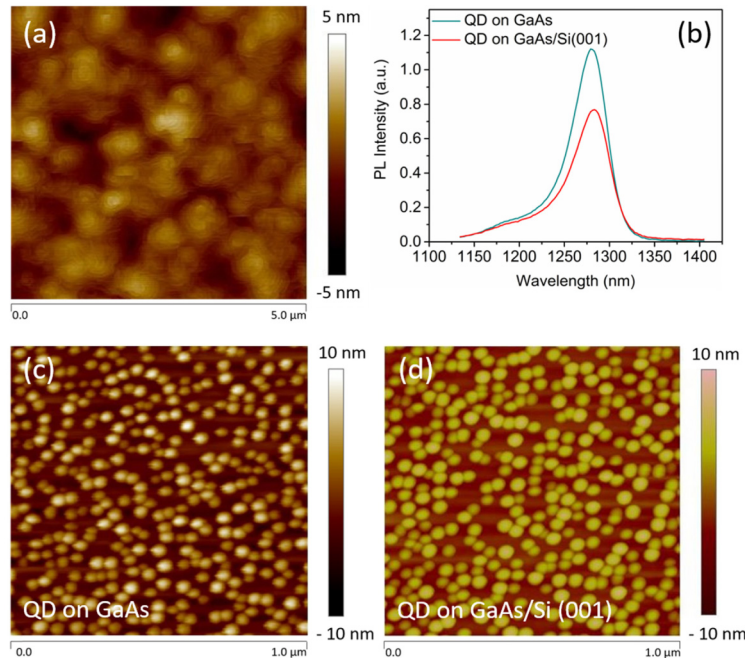


Fig. 2. (a)  $5 \times 5 \mu\text{m}^2$  AFM image of a 400 nm GaAs film layer direct grown on the nominal Si (001) substrate. (b) PL comparison of 5-layer InAs/GaAs QD laser structure grown on GaAs/Si (001) to a reference sample grown on GaAs substrate at room temperature under the same pump conditions. (c)-(d)  $1 \times 1 \mu\text{m}^2$  AFM images of uncapped InAs/GaAs QDs grown on native GaAs and GaAs/Si (001) substrates, respectively.

### 3. Epitaxial InAs/GaAs QD laser structure on GaAs/Si (001)

Figure 2(a) shows a typical  $5 \times 5 \mu\text{m}^2$  AFM image of a 400 nm thick GaAs film layer monolithically grown on a 300 mm industry-compatible Si (001) substrate by MOCVD based on the process described above. The measured AFM image indicates that a small RMS surface roughness of 0.86 nm has been achieved, and this very small surface roughness is comparable to the best reported values for 1  $\mu$ m thick GaAs layers grown on Si (001) substrate with  $4^\circ - 6^\circ$  offcuts [33, 34], despite the fact that only 400 nm GaAs has been deposited on the nominal (001) Si substrate in our structure. In addition, no obvious “V” – groove feature can be observed indicating the realization of an APB-free surface due to the formation of perfect doubling of the height of all silicon surface steps thanks to the effective Si wafer preparation [31]. The observations of APB-free heteroepitaxial GaP on Si (001) by MOCVD have been reported by W. Stolz’s group [27, 35]. In their work, to achieve the APB-free GaP/Si (001) substrate, a homoepitaxial silicon buffer along with a high temperature annealing process is required prior to GaP heteroepitaxy. In comparison, the method presented in the present work is simpler and more compatible with standard industry fabrication processes, since our process does not require the additional Si buffer growth and annealing process or the use of a GaP layer prior to GaAs growth.

In addition, room temperature PL was employed to compare the optical properties of the QD laser structures grown on nominal GaAs/Si (001) and on native GaAs substrates. As shown in Fig. 2(b), the two samples present similar room temperature emission peaks at  $\sim 1285$  nm and linewidths of  $\sim 32$  meV. The PL intensity is quite comparable, with the reference QD sample having an integrated PL intensity  $\sim 1.3$  times greater than that of the sample grown on nominal GaAs/Si (001). An AFM comparison of uncapped InAs QDs grown on nominal GaAs/Si (001) and on native GaAs substrate is shown in the Figs. 2(c) and 2(d), revealing similar morphologies. Both samples present good uniformity and the dot density determined by AFM is  $\sim 3.5 \times 10^{10} \text{ cm}^{-2}$  and  $\sim 3 \times 10^{10} \text{ cm}^{-2}$  for samples grown on GaAs/Si (001) and on native GaAs substrates, respectively.

#### 4. Results and discussion

Figure 3(a) compares light-current-voltage (LIV) characteristics of InAs/GaAs QD lasers grown on GaAs/Si (001) and native GaAs substrates, respectively, under cw operation at room temperature. As expected, the measured series resistances extracted from IV characteristics for both samples were quite similar at round  $1.9 \pm 0.2 \Omega$ , since the doping levels of the laser structure and the fabrication procedures were nominally identical. The measured lasing threshold current densities are  $210 \text{ A/cm}^2$  and  $425 \text{ A/cm}^2$  for GaAs-based and Si-based devices, respectively. The calculated slope efficiency and external differential quantum efficiency is  $0.12 \text{ W/A}$  and  $12.7\%$  for GaAs-based device, and  $0.068 \text{ W/A}$  and  $7.2\%$  for the Si-based laser. Compared with the laser device grown on native GaAs substrate, the degraded device performances for QD laser grown on the Si (001) substrate is related to the defects propagating into the QD active layers. Figure 3(b) compares the room temperature single facet output power against the current density for InAs/GaAs QD laser grown on GaAs/Si (001) substrate under cw and pulsed conditions. Under cw operation, a maximum single facet output power of  $43 \text{ mW}$  is obtained at an injection current density of  $1332 \text{ A/cm}^2$  due to the limitation of the cw current source. However, a small thermal rollover of output power at high injection current densities is observed. In contrast, under pulsed operation, a maximum single facet output power of over  $134 \text{ mW}$  is achieved at an injection current density of  $2 \text{ kA/cm}^2$  without any thermal rollover.

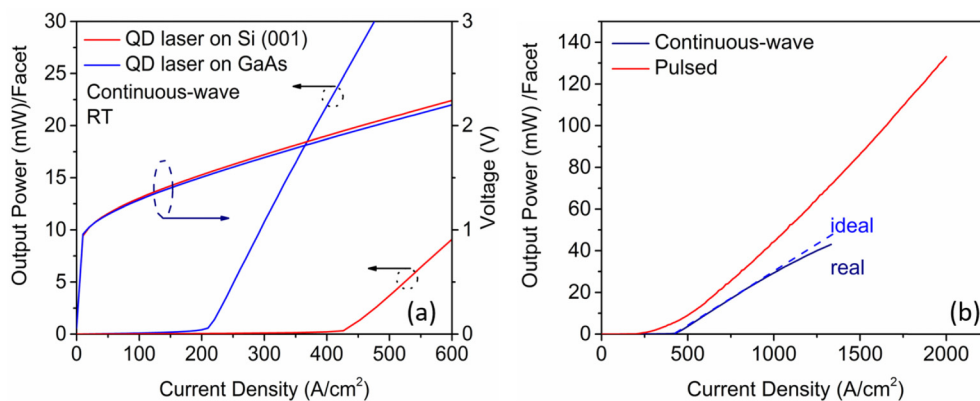


Fig. 3. (a) LIV characteristics comparison of InAs/GaAs QD laser grown on GaAs/Si (001) to the reference QD laser grown on native GaAs substrate at room temperature under cw operation. (b) LI comparison of InAs/GaAs QD laser grown on GaAs/Si (001) substrate under c.w and pulsed operation conditions at room temperature.

Figure 4 shows the evolution of the emission spectra as a function of injected current densities under cw operation at room temperature. A spontaneous emission spectrum with a broad full width at half maximum (FWHM) of  $49 \text{ nm}$  is observed at a peak wavelength of  $\sim 1292 \text{ nm}$  at a relatively low driven current density of  $267 \text{ A/cm}^2$ . On increasing the injection

current density to  $425 \text{ A/cm}^2$ , a typical lasing oscillation behavior, evidenced by sudden spectrum narrowing to  $\sim 2.2 \text{ nm}$  (as seen in the inset of Fig. 4) and a sharp increase in intensity, is observed. Further increasing the current density, an obvious multi-mode lasing spectrum appears.

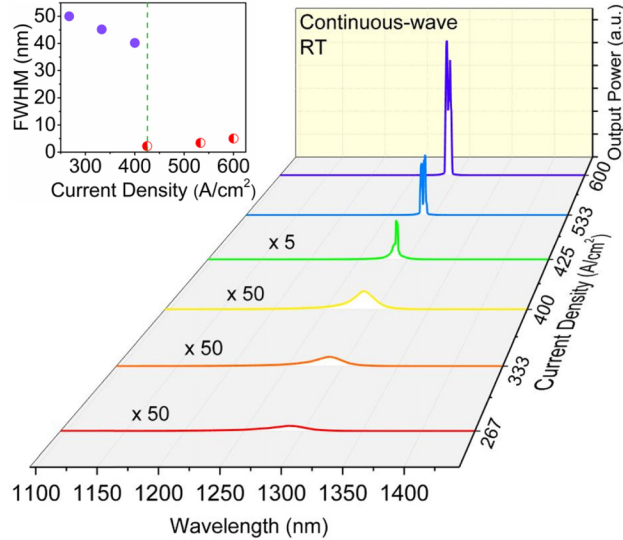


Fig. 4. Emission spectra for InAs/GaAs QD laser on GaAs/Si (001) substrate at various injection current densities at room temperature. The inset shows the evolution of the FWHM as a function of injection current density.

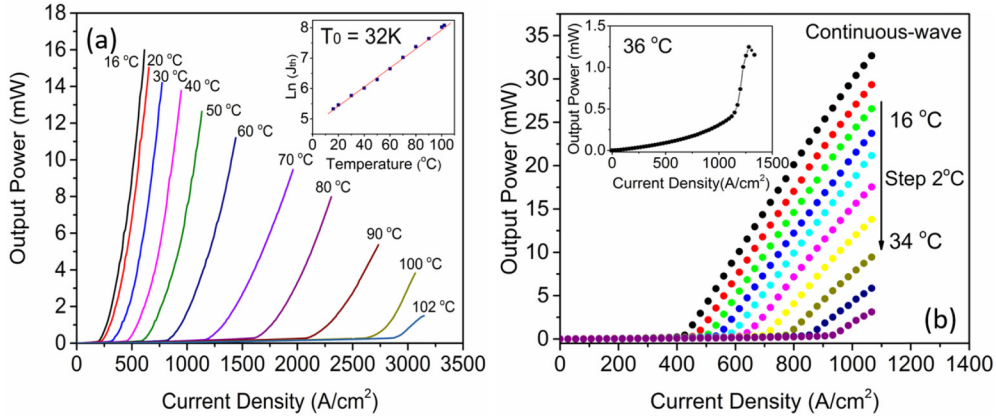


Fig. 5. Single facet light power versus current density for a Si-based InAs/GaAs QD laser grown on GaAs/Si (001) substrate at various heat sink temperatures under pulsed condition. The inset shows the natural logarithm of current density against temperature in the ranges of 16 – 102 °C. (b) Single facet output power versus current density for the same Si-based InAs/GaAs QD laser as a function of temperature under cw operation. The inset shows the LI curve for this Si-based InAs/GaAs QD laser at a heat sink temperature of 36 °C.

Figure 5(a) shows the LI characteristic of InAs QD laser grown on GaAs/Si (001) substrate at various heatsink temperatures under pulsed mode. This Si-based QD laser has a maximum heatsink temperature of 102 °C for lasing operation, with a characteristic temperature,  $T_0$ , of  $\sim 32 \text{ K}$  between 16 °C and 102 °C. To the best of knowledge, this is the first demonstration of QD lasers monolithically grown on exact silicon (001) substrate that lase over to 100 °C. The temperature-dependent LI characteristics have also been measured

under cw operation, as shown in Fig. 5(b). Under cw operation, this device has a maximum heatsink temperature of 36 °C for lasing operation. As seen from the inset of the Fig. 5(b), at a heatsink temperature of 36 °C, there is a strong thermal output power rollover due to the self-heating of the device, which severely limits its high temperature performance. It should be mentioned that the QD active region employed in this work is undoped; also the laser device was not hard soldered to a high thermal-conductivity heatsink. The relative poor  $T_0$  value presented here is therefore mainly related to the hole excitation out of the lowest lasing state [36] and imperfect heat extraction strategy. A next step towards improving the temperature performance and maximum output power will be concerned with reducing the temperature sensitivity and optimizing the extraction of heat from the active region. The well-established strategies to achieve this is modulation p-doping of the QDs [12, 36] or/and hard soldering the laser to a high-thermal-conductivity heatsink.

Comparing the present results grown on on-axis Si (001) substrates with the world-record results of InAs/GaAs QD lasers grown directly on offcut Si substrates [24], there has been observed degradation in laser performance for this work, including higher threshold current densities and poorer  $T_0$ . We must emphasize that, the growth on Si (001) substrates is not fully optimized due to limitations on the wafer preparation and the MBE growth chamber was in sub-optimal condition with significant numbers of oval defects visible. Nevertheless, good c.w. performance has been achieved, and the threshold current density reported in the present work has been reduced by more than a factor of two, compared with the very recent achievement of an InAs/GaAs QD laser on on-axis Si (001) substrate with an intermediate GaP buffer layer [30]. With further optimization on the wafer preparation and the growth of dislocation filter layers [17], even better results are to be expected.

## 5. Conclusion

In conclusion, we have demonstrated the first electrically pumped cw InAs/GaAs QD lasers directly grown on industrial-compatible nominal Si (001) substrates without any intermediate buffers. The devices exhibit cw lasing at  $\sim 1.3 \mu\text{m}$  with threshold current density of  $425 \text{ A/cm}^2$  and output of 43 mW at room temperature. Under pulsed operation, we show significantly improved device performance including lasing operation at device temperatures exceeding 100 °C and output from a single facet exceeding 130 mW at room temperature by limiting self-heating. These results represent a major advance towards the commercial success of silicon-based photonic-electronic integration.

## Funding

UK Engineering and Physical Sciences Research Council (EP/J012904/1, EP/K029118/1, and EP/P006973/1).

## Acknowledgments

The authors want to thank RENATECH program, CEA-Leti Minatec clean room staff and especially Y. Bogumilowcz, and Applied Materials for Fruitful discussion.